Osmaniye Korkut Ata Üniversitesi
Fen Bilimleri Enstitüsü Dergisi
Cilt 3, Sayı 2, 135-145, 2020

Osmaniye Korkut Ata University
Journal of Natural and Applied Sciences
Volume 3, Issue 2, 135-145, 2020

Osmaniye Korkut Ata Üniversitesi Fen Bilimleri Enstitüsü Dergisi

Osmaniye Korkut Ata University Journal of Natural and Applied Sciences

Eğilme Etkisindeki Dikdörtgen Delik İçeren FDM Şerit-Plağın Statik Analizi

Ülkü BABUŞCU YEŞİL[1*], Melis GEZER[2]

[1,2]Yildiz Technical University, Faculty of Chemical and Metallurgical Engineering, 34210, Istanbul

[1] https://orcid.org/0000-0002-8557-8308
[2] https://orcid.org/0000-0001-9823-8292
*Sorumlu yazar: ubabuscu@yildiz.edu.tr

Araştırma Makalesi

Makale Tarihçesi:
Geliş tarihi: 2 Eylül 2020
Kabul tarihi:13 Ekim 2020
Online Yayınlanma:15 Aralık 2020

Anahtar Kelimeler:
Fonksiyonel Derecelendirilmiş Malzeme
Dikdörtgen Delik
Statik Analiz
SEM

ÖZET

Bu çalışmada, eğilme kuvveti etkisinde basit mesnetli dikdörtgen delik içeren FDM şerit plak incelenmiştir. Young modülü şerit plağın uzunluğu ve genişliği boyunca kuvvet yasası fonksiyonlarına göre değişirken Poisson oranı ve materyal yoğunluğu sabit kabul edilmiştir. Teorik incelemenin modellenmesinde klasik lineer elastisite teorisi ve genelleştirilmiş düzlem-şekil değiştirme koşulları ele alınmıştır. Problemin nümerik çözümü Sonlu Elemanlar Metodu (SEM) ile elde edilmiştir. Çözüm bölgesinin ayrıklaştırılmasında sonlu sayıda alt bölge kullanılmıştır ve her alt bölgedeki çözüm bir polinom fonksiyonu olarak düşünülmüştür. Sınır değer probleminin SEM modellemesi, Ritz tekniği ile yapılmıştır. Çözüm bölgesi belirli bir sayıda 9 düğüm içeren dikdörtgen elemanlar ile ayrıklaştırılmıştır. SEM modellemesi için yer değiştirme temelli sonlu elemanlar kullanılmıştır. Deliğin FDM şerit plağın üzerindeki etkisini anlamak için yer değiştirme ve gerilme yayılımlarının sonuçları incelenmiştir.

Static Analysis of FGM Plate-Strip with a Rectangular Hole Under Bending

Research Article

Article History:
Received: 2 September 2020
Accepted: 13 October 2020
Published online: 15 December 2020

Keywords:
Functionally Graded Material
Rectangular Hole
Static Analysis
FEM

ABSTRACT

In this sudy, a simply supported FGM plate-strip with rectangular hole subjected to bending loadings is investigated. Young's modulus varies continuously throughout the length and width of the plate-strip based on the power-law functions; but the Poisson's ratio and material density are assumed to be constant. The classical linear elasticity theory and the generalized plane-strain conditions are assumed for the modelling of the theoretical investigations. The solution of the considered problem is obtained numerically with the help of the Finite Element Method (FEM). Finite number of sub-domains (FEs) are used for the discretization of the solution domain and the solution in each sub-domain is considered as a polynomial function. Employing the Ritz technique, the FEM modelling of the boundary value problem is obtained. The solution domain is discretized a certain number of rectangular elements having nine nodes. We have used displacement-based finite elements for the FEM modelling. The solutions of the displacement and stress concentration are investigated to understand the hole effect on the plate-strip made of functionally graded materials.

To Cite: Yeşil ÜB., Gezer M. Static Analysis of FGM Plate Strip with a Rectangular Hole Under Bending. Osmaniye Korkut Ata Üniversitesi Fen Bilimleri Enstitüsü Dergisi 2020; 3(2): 135-145.

1. Introduction

Displacement and stress concentrations in structures with geometrical discontinuities in the form of holes and cutouts have received wide attention in the literature in that they cause of failure. The problem widely investigated, and several analytical, experimental, and numerical techniques have existed for the reduction of the stress concentration around discontinuities for homogeneous materials.

The first and systematic studies in this area were done by Savin [1]. Savin analyzed the distributions of displacements and stresses for infinite plates with holes of different geometry, with the help of complex functions theory and conformal transformation analytically under various stress boundary conditions. For the rectangular hole, the conformal transformation function that converts the outside of the rectangular hole into the unit circle is expressed as an infinite series. Stress functions for the finite number term of this series are obtained analytically. Taking the finite number of terms from the conformal transformation series, this piece refers to the transformation for the hole with a rounded geometry rather than a real rectangular hole. Obtaining the rectangular hole form and obtaining a sufficiently accurate result for the stress distributions at the corner points requires taking too many terms from the conform transformation function. Until now, only a few terms from this series have been studied in Savin [1] and Jong [2] for analyzing stress and displacement distributions. These results are far from the actual values in the regions near the corner points. Rao et al. [3] gave analytical solutions to get the stress distribution around the square and rectangular cutouts edges of which are reasonably straight, and the corners are rounded without sharp corners.

In Lei et al. [4] the solution technique given above was tried to be developed and by taking a few terms from the conform transformation function, a correction coefficient was included in the processes, the method given in Savin [1] was developed and results were given for infinite isotropic plates. The form of a rectangular hole with sharp corners has been addressed in Yahnioğlu and Yücel [5] for isotropic plate-strip.

Recently, FGM has been widely used in many engineering applications for reducing stress concentrations by taking advantage of their material inhomogeneity. FGM possesses continuously varying microstructure and mechanical properties. There are no internal boundaries that exist, and the interfacial stress concentrations can be avoided. There are several studies on graded material structures including beams, plates, shells, and cylinders, with and without discontinuities.

Some plane elasticity problems and analytical solutions were given for plates made of FGM with and without cracks under different boundary conditions in Erdoğan and Wu [6]. Graded finite elements were formulated using linear interpolation functions in Santare and Lambros [7]. Graded finite elements were presented using a generalized isoparametric formulation in Kim and Paulino [8]. A comprehensive review of FGM has been made in Udupa et al. [9]. Stress concentration in an infinite panel having a rounded rectangular hole reinforced with a functionally graded material layer using the extended finite element method [10].

In the present paper within the two dimensional (2D) finite element method (FEM) modeling of a plate-strip made functionally graded material (FGM) with a rectangular hole with sharp corners is studied and the effect varying material properties of FGM on the concentrations of static displacements and stresses caused by the bending loading is investigated.

Numerical results are compared with the corresponding numerical values of isotropic plates and with the whole plate made functionally graded material.

2. Mathematical Formulation of the Problem

The geometry and loading of the plate-strip are given in Figure 1.

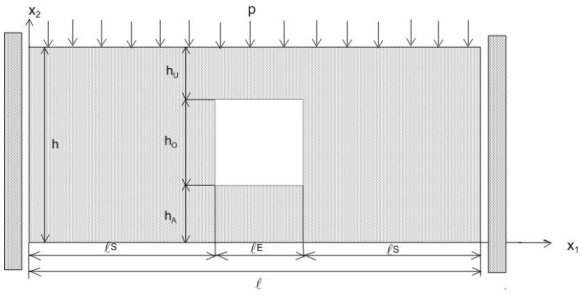

Figure 1. Loading of the plate-strip with a rectangular hole

Young's modulus of the medium varies continuously in the horizontal and vertical directions according to power law distribution, but the Poisson's ratio and material density are assumed to be constant. The following functional forms are used for the nodal values of Young's modulus through the axes Ox_1 and Ox_2 respectively.

$$E(x_1,x_2)=E(x_1)=E_0(ax_1+b)^n$$
$$E(x_1,x_2)=E(x_2)=E_0(cx_2+d)^n \;\; E_0,a,b,c,d,n\in R \tag{1}$$

where E_0 is the Young's modulus at x_i=0, i=1,2 and n is the exponent of the power law material variation. These problems are solved for a half of the domain, because of the symmetry of the geometry and loading with respect to the planes $x_1=\ell/2$**.** The material property gradient around the rectangular hole for the half of the solution domain is shown for the Problem 1 (Problem 2) in Figure 2a (Figure 2b).

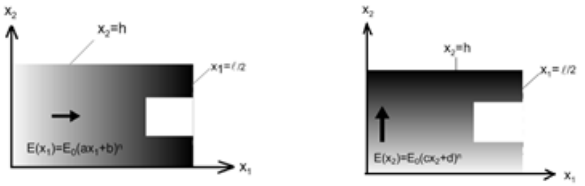

(a) **(b)**

Figure 2. Half FGM plate-strip with material properties varying over **(a)** Ox_1 axis (Problem 1) and, **(b)** Ox_2 axis (Problem 2)

The classical linear elasticity theory and the generalized plane-strain conditions are assumed for the modeling of the theoretical investigations [11]. Solution domain of boundary value problem is;

$$W'=W-W_h$$
$$W=\{0\le x_1\le \ell;0\le x_2\le h\}$$
$$W_h=\{\ell_S\le x_1\le \ell_S+\ell_E;h_A\le x_2\le h_A+h_O\} \tag{2}$$

The solution of the considered problem is obtained numerically with the help of the Finite Element Method (FEM). Finite numbers of sub-domains (FEs) are used for the discretization of the solution domain and the solution in each sub-domain is considered as a polynomial function. The displacement functions of the FGM plate-strip for each finite element can be written as;

$$\begin{Bmatrix}u_1^{(e)}\\u_2^{(e)}\end{Bmatrix}=\sum_{i=1}^{n}N_i\begin{Bmatrix}u_{1i}^{(e)}\\u_{2i}^{(e)}\end{Bmatrix};e=1,2,...,M \tag{3}$$

where N_i is the shape function, u_{ki} is the nodal displacement corresponding to node i in the k direction, n is total number of nodal points in the element; M is total number of finite elements in the solution domain. Also strain functions can be derived from displacements by differentiation as

$$\varepsilon^{(e)}=B^{(e)}u^{(e)} \tag{4}$$

where $B^{(e)}$ is the displacement-strain matrix of shape function derivatives and $u^{(e)}$ is the nodal displacement vector. Equations and relations can be determined by solving the boundary value problem.

$$\frac{\partial\sigma_{ij}}{\partial x_j}=0;\sigma=D(x_1,x_2)\varepsilon;$$
$$\sigma=[\sigma_{11},\sigma_{22},\tau_{12}];\;\varepsilon=[\varepsilon_{11},\varepsilon_{22},\gamma_{12}];$$
$$\varepsilon_{ij}=\frac{1}{2}\left(\frac{\partial u_i}{\partial x_j}+\frac{\partial u_j}{\partial x_i}\right),\ \text{i,j=1,2;}$$
$$u_2\big|_{\substack{x_1=0,\ell\\x_2\in[0,h]}}=0;\;\sigma_{i2}\big|_{\substack{x_2=h\\x_1\in[0,\ell]}}=p\delta_i^2;$$
$$\sigma_{i2}\big|_{\substack{x_2=0\\x_1\in[0,\ell]}}=0;\sigma_{11}\big|_{\substack{x_1=0,\ell\\x_2\in[0,h]}}=0;$$
$$\sigma_{ij}n_j\big|_{w_h}=0,\ \text{i,j=1,2} \tag{5}$$

In (5) $D(x_1, x_2)$ is the constitutive matrix, which is a function of position of points. So, this matrix's form for each finite element will be $D_{ij}^{(e)}=D_{ij}^{(e)}(x_1)$ (for problem 1) and $D_{ij}^{(e)}=D_{ij}^{(e)}(x_2)$ (for Problem 2). The elements of this matrix can be given for the constant Poisson ratio;

$$D_{11}=D_{22}=\frac{(1-\upsilon)E(x_i)}{(1+\upsilon)(1-2\upsilon)},\ D_{12}=D_{21}=\frac{\upsilon E(x_i)}{(1+\upsilon)(1-2\upsilon)},\ D_{66}=\frac{E(x_i)}{2(1+\upsilon)} \tag{6}$$

where i=1 (2) for Problem 1(2).

3. Fem Modelling of the Problem

For the FEM modelling of the boundary value problem, total potential energy functional Π is used.

$$\Pi=\frac{1}{2}\iint_{W'}\sigma_{ij}\varepsilon_{ij}dx_1dx_2-\int_0^{\ell}pu_2\big|_{x_2=h}dx_1,\ \text{i,j=1,2} \tag{7}$$

where W' is the solution domain. Employing the Ritz technique, we are obtained the FEM modelling of the boundary value problem from the equation $\delta\Pi=0$ [11]. Solution domain is discretized into a certain number of finite

elements. Finite elements are chosen as rectangular elements with 9 nodes (Figure 3).

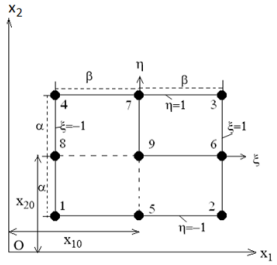

Figure 3. Nodes of representative finite element.

Expressions of the 2nd order Standard Lagrange Shape functions which are defined on the rectangular finite elements at normalized coordinates ($O'\xi\eta$) are: [11]

$$\begin{aligned}
&N_1=\frac{1}{4}\left(\xi^2-\xi\right)\left(\eta^2-\eta\right),\ N_2=\frac{1}{4}\left(\xi^2+\xi\right)\left(\eta^2-\eta\right),\\
&N_3=\frac{1}{4}\left(\xi^2+\xi\right)\left(\eta^2+\eta\right),N_4=\frac{1}{4}\left(\xi^2-\xi\right)\left(\eta^2+\eta\right),\\
&N_5=\frac{1}{4}\left(\xi^2-1\right)\left(\eta^2-\eta\right),\ N_6=-\frac{1}{2}\left(\xi^2+\xi\right)\left(\eta^2-1\right),\\
&N_7=-\frac{1}{2}\left(\xi^2-1\right)\left(\eta^2+\eta\right),\ N_8=-\frac{1}{2}\left(\xi^2-\xi\right)\left(\eta^2-1\right),\\
&N_9=\left(\xi^2-1\right)\left(\eta^2-1\right)
\end{aligned} \tag{8}$$

The relation which provide the transformation between the local coordinate system $O'\xi\eta$ and the natural coordinate system Ox_1x_2 is:

$$\xi=\frac{x_1-x_{10}}{\beta},\ \eta=\frac{x_2-x_{20}}{\alpha} \tag{9}$$

The same discretization of finite element is used for finite element solution of each boundary value problem. The displacement function on each finite element is chosen as polynomial function as given in (3). This expression is substituted in the functional (7). When the required operations are done, the solution is reduced to

$$Ku=F \tag{10}$$

Here, K is the stiffness matrix, u is the vector which contains unknowns on the nodes and F is the force vector. For example, K elements for any chosen e^{th} finite element.

$$K^e=\int_{W^{(e)}}\left(B^{(e)}\right)^T D^{(e)}\left(x_k\right)B^{(e)}d\Omega_e \tag{11}$$

where $W^{(e)}$ $W'=\bigcup_{e=1}^{M} W^{(e)}$ is the domain of e^{th} finite element and T indicates transpose, be $D_{ij}^{(e)}=D_{ij}^{(e)}(x_1)$ (for problem 1) and $D_{ij}^{(e)}=D_{ij}^{(e)}(x_2)$ (for Problem 2). Gaussian Quadrature Method which is one of the numerical integration methods is used to calculate elements of the matrix with 10 sample points for each finite element. The same finite element discretization is used in finite element solution of both problems. All computer programs used for numerical investigations carried out have been composed by the authors in the package FTN77.

4. Numerical Results

Due to the symmetry about the plane $x_1/\ell=1/2$ only one half of the full plate-strip is under consideration. The solution domain discretized into 80 and 12 rectangular finite elements along the Ox_1 and Ox_2 axes, respectively. FE discretization of the solution domain is selected among the finite element meshes in which the numerical results found for many finite elements' meshes are best approached to the corresponding numerical results in the literature. It should be noted that the graphs of the displacements and stresses obtained for the Problem 1 (Problem 2) are given according to the axis Ox_1 (Ox_2). In the present study, Poisson's ratio is assumed to be constant and set to be $\nu=0.3$.

The solution domain is discussed as 4 cases with respect to different sizes of the hole. The following dimension of hole are used for W_h given in equation (12),

$$\begin{aligned}
&\text{Case 0: } W'=W \text{ where } W=\left\{0\le x_1\le\frac{\ell}{2};\ 0\le x_2\le h\right\}\\
&\text{Case 1: } W'=W-W_h \text{ where } W_h=\left\{\frac{3\ell}{8}\le x_1\le\frac{\ell}{2};\ \frac{h}{3}\le x_2\le\frac{2h}{3}\right\}\\
&\text{Case 2: } W'=W-W_h \text{ where } W_h=\left\{\frac{\ell}{4}\le x_1\le\frac{\ell}{2};\ \frac{h}{3}\le x_2\le\frac{2h}{3}\right\}\\
&\text{Case 3: } W'=W-W_h \text{ where } W_h=\left\{\frac{\ell}{8}\le x_1\le\frac{\ell}{2};\ \frac{h}{3}\le x_2\le\frac{2h}{3}\right\}
\end{aligned} \tag{12}$$

where ℓ is the length of the plate-strip and h is the width of the plate-strip.

The main aim of the present numerical investigations is to determine how the functional material property effect the stress and displacement concentrations for the different size of the rectangular hole under bending. Before considering the main numerical results, for testing of the used calculation algorithm and programs which are composed by the authors and realized in FORTRAN 77, plate-strip without a hole is considered.

Figure 4 illustrates the distribution of σ_{11}/p of the plate-strip without a hole (Case 0) which is

under bending force for Problem 1 at x_2=h and for Problem 2 at $x_1 = \ell/4$. E_1/E_0 represents the variation of Young modulus due to the use of dimensionless sizes. E_0 (E_1) is the Young's modulus at x_i=0, i=1, 2 (x_1=ℓ/2 or x_2=h). Choosing $E_1/E_0 = 1$ corresponds that plate-strip material is homogeneous.

Figure 4a shows that material property of plate-strip approximates the homogeneous state with decreasing of E_1/E_0 and the graph is coincident with analytical solution given in [12]. Also, Figure 4.b illustrates that FEM solutions for each value of E_1/E_0 identical the analytical solutions given in [6], in the case that plate-strip has FGM property in the direction of Ox_2. These results indicate sensitivity and accuracy of finite element algorithms we constituted. So, the verification of the algorithm and the programs used for determining the numerical results has been completed.

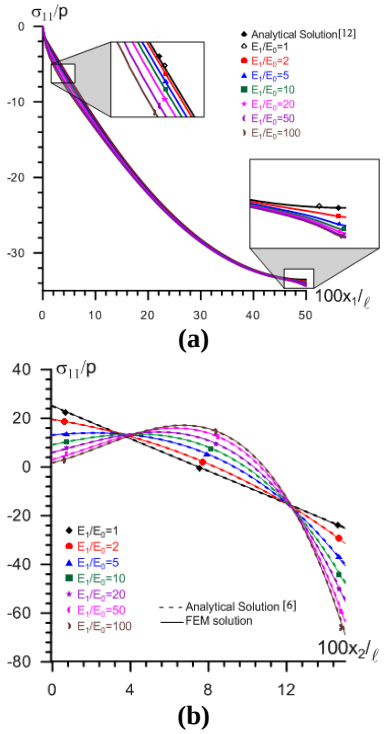

Figure 4. For plate-strip without rectangular hole, effect of changing E_1/E_0 to the distribution of σ_{11}/p for n=2 for **(a)** Problem 1 **(b)** Problem 2.

The distribution of σ_{11}/p for various values of the material nonhomogeneity parameter E_1/E_0 for the three cases versus Case 0 on the plane x_2=h for Problem 1 are plotted in Figure 5. Figure 5 shows that the more E_1/E_0, the larger absolute values of the stresses of σ_{11}/p. The difference between the values obtained for Case 0 and the other cases also increase with the size of the hole. As the size of the hole increases, the difference between the values of the stresses of σ_{11}/p for FGM and homogeneous plate (E_1/E_0=1) increases and as the size of the hole increases tensile stress occurs.

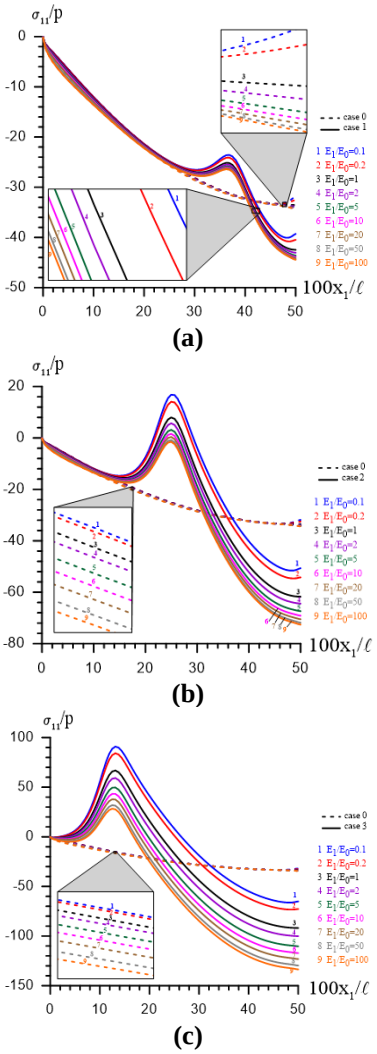

Figure 5. The normalized stress of σ_{11}/p at x_2=h plane for different values of E_1/E_0 for n=2 for (a) Case 1 (b) Case 2 (c) Case 3 versus Case 0 for Problem 1.

Fig. 6 represents the distribution of σ_{11}/p for various values of the material non homogeneity parameter E_1/E_0 for three cases versus Case 0 on the plane $x_1 = \ell_s/2$ for Problem 2 along the Ox_2 axis. The maximum tensile stress is at the bottom edge $x_2/\ell = 0$ for $E_1/E_0 \le 2$ and the maximum compressive stress is at the top surface at $x_2/\ell = h$ for $E_1/E_0 \ge 1$ for Case 1 and Case 2. For the ratio E_1/E_0=1 in which the FGM plate becomes a homogeneous plate, the stress concentration is a linear function of x_2 and the maximum stress is at the top or bottom surface of the plate for Case 1 (in Figure 6a) and Case 2 (in

Figure 6b), but for Case 3 (in Figure 6c) it is not linear because of the hole and edge effects.The difference between the values obtained for Case 0 and the other Cases also increase with the size of the hole.

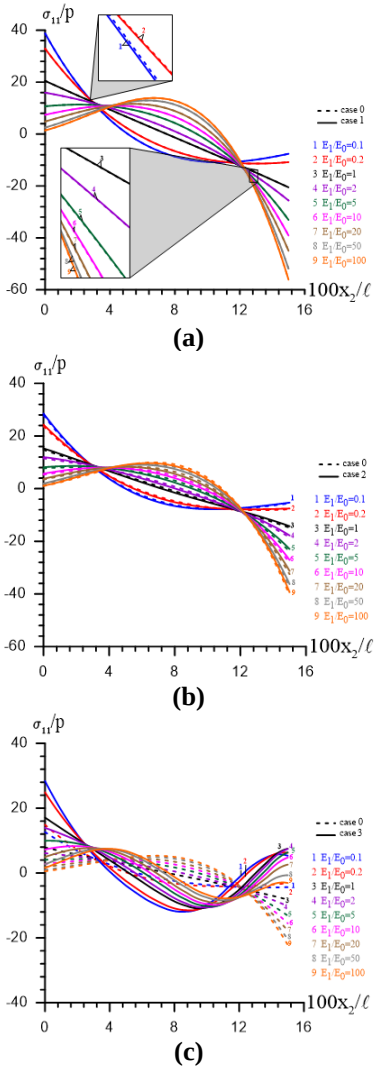

Figure 6. The normalized stress of σ_{11}/p at $x_1 = \ell_s/2$ plane for different values of E_1/E_0 for n=2 for (a) Case 1 (b) Case 2 (c) Case 3 versus Case 0 for Problem 2.

Figure 7 illustrates the distribution of τ_{12}/p for various values of the material non homogeneity parameter E_1/E_0 for the three cases versus Case 0 on the plane $x_1 = \ell_s/2$ for Problem 2. It follows from the graphs that the absolute values of the stresses of τ_{12}/p decrease with increasing the parameter E_1/E_0 for the first half of the width (i.e., [0, h/2]), while increase with increasing the parameter E_1/E_0 for the second half of the width [h/2,h] for Cases 0, 1 and 2 (in Figure 7a and Figure 7b) but for Case 3 (in Figure 7c) absolute values of τ_{12}/p decrease with increasing the parameter E_1/E_0. The difference between the values of the stresses of τ_{12}/p obtained for Case 0 and the other Cases also increase with the size of the hole in Problem 2. The maximum difference occurs for the Case 3 and Case 0 (in Figure 7c).

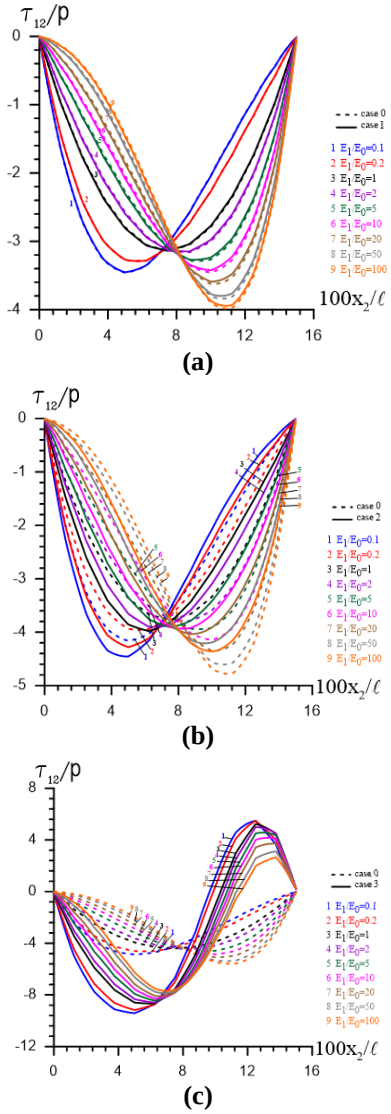

Figure 7. The normalized stress of τ_{12}/p at $x_1 = \ell_s/2$ plane for different values of E_1/E_0 for n=2 for (a) Case 1 (b) Case 2 (c) Case 3 versus Case 0 for Problem 2

Figure 8 illustrates the distribution of σ_{22}/p for various values of the material non homogeneity parameter E_1/E_0 for three Cases versus Case 0 on the plane $x_2=5h/6$ for Problem 1. The graphs indicate that the absolute values of the stresses of σ_{22}/p decrease with increasing the parameter E_1/E_0 for the Problem 1, and maximum effect occur around the hole region. It can be said that compressive stress occur at edge and center of the plate-strip with changing parameter E_1/E_0 for Case 0 in Problem 1.

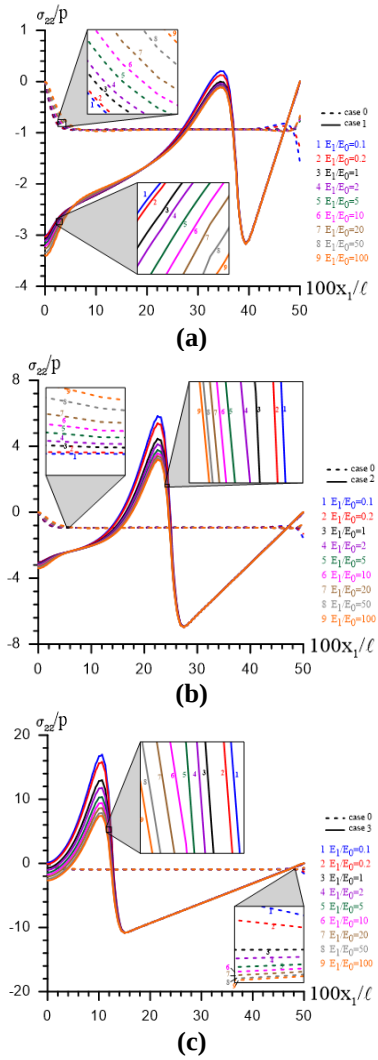

Figure 8. The normalized stress of σ_{22}/p at x_2=5h/6 plane for different values of E_1/E_0 for n=2 for (a) Case 1 (b) Case 2 (c) Case 3 versus Case 0 for Problem 1.

Figure 9 illustrates the distribution of σ_{22}/p for various values of the material non homogeneity parameter E_1/E_0 for the three Cases versus Case 0 on the plane $x_1 = \ell_s/2$ for Problem 2. The graphs indicate that the absolute values of the stresses of σ_{22}/p decrease with increasing the parameter E_1/E_0 for the Problem 2 and the difference between the values obtained for Case 0 and the other Cases also increase with the size of the hole. The maximum difference occurs for the Case 3 and Case 0. Also, tensile stress is observed in Cases 2 and 3 (in Figure 9b and Figure 9c) as only compressive stress occur in Case 0 and 1 (in Figure 9a)

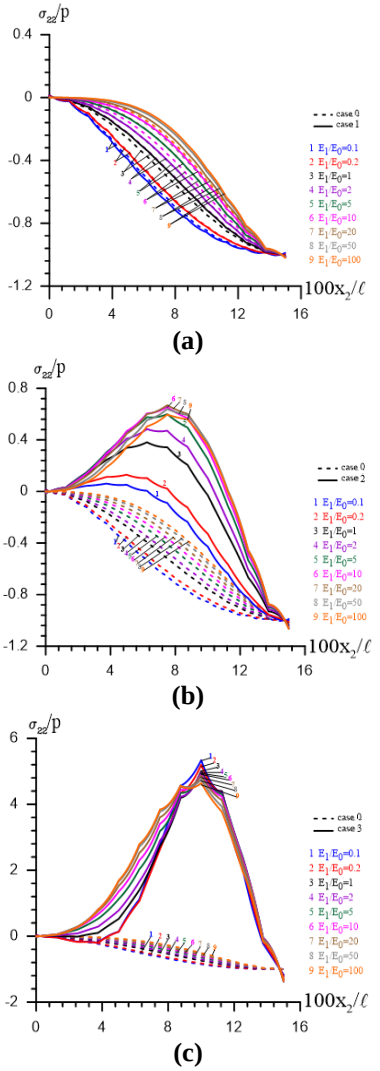

Figure 9. The normalized stress of σ_{22}/p at $x_1 = \ell_s/2$ plane for different values of E_1/E_0 for n=2 for (a) Case 1 (b) Case 2 (c) Case 3 versus Case 0 for Problem 2.

Figure 10 represents the distribution of $u_1E_0/p\ell$ for various values of the material non homogeneity parameter E_1/E_0 for three cases versus Case 0 on the plane x_2=h for Problem 1. It follows from the graphs that the absolute values of the displacement of $u_1E_0/p\ell$ decrease with increasing the parameter E_1/E_0. The difference between the values of the displacements of $u_1E_0/p\ell$ obtained for Case 0 and the other Cases also increase with the size of the hole, and this difference is more for E_1/E_0<1 than E_1/E_0>1.

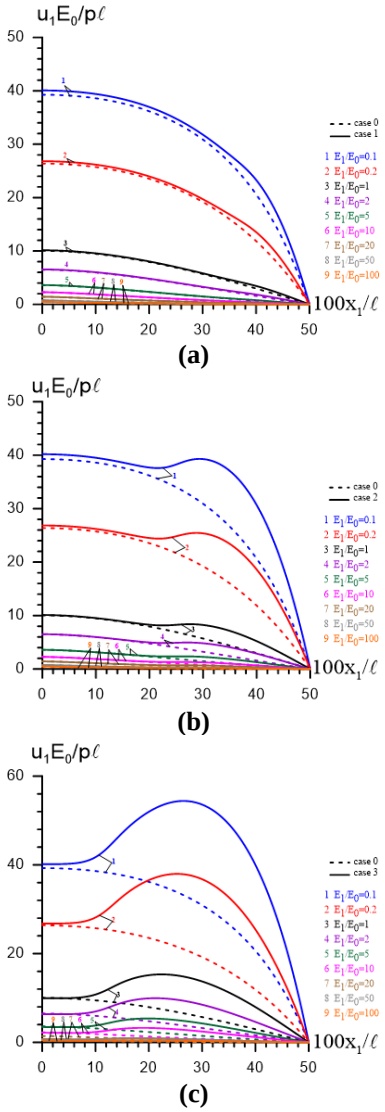

Figure 10. The normalized displacement of $u_1E_0/p\ell$ at x_2=h plane for different values of E_1/E_0 for n=2 for (a) Case 1 (b) Case 2 (c) Case 3 versus Case 0 for Problem 1

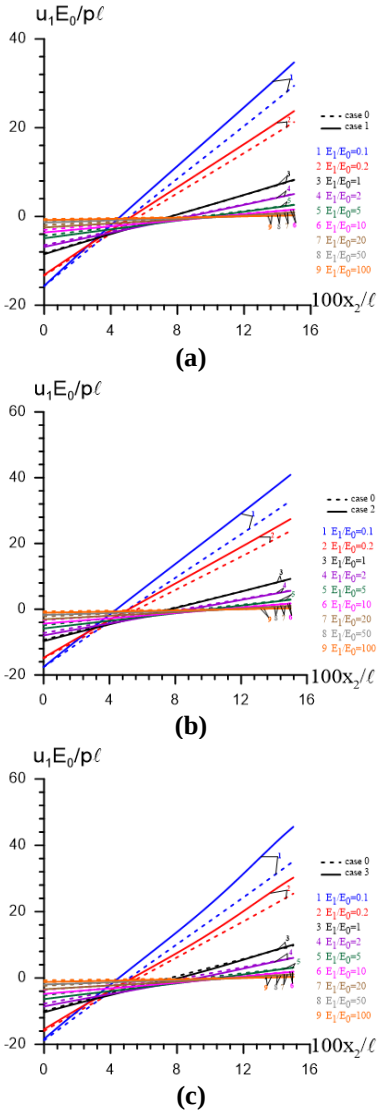

Figure 11. The normalized displacement of $u_1E_0/p\ell$ at $x_1 = \ell_s/2$ plane for different values of E_1/E_0 for n=2 for (a) Case 1 (b) Case 2 (c) Case 3 versus Case 0 for Problem 2.

Figure 11 represents the distribution of $u_1E_0/p\ell$ for various values of the material non homogeneity parameter E_1/E_0 for three cases versus Case 0 on the plane $x_1 = \ell_s/2$ for Problem 2. The displacement of $u_1E_0/p\ell$ of the FGM plate is linear for Problem 2. It is observed that the absolute values of displacement decreases upon increasing E_1/E_0.

The distribution of $u_2E_0/p\ell$ for various values of the material non homogeneity parameter E_1/E_0 for the three cases versus Case 0 on the plane x_2=h for Problem 1 are plotted in Figure 12. The graphs show that the absolute values of the displacements of $u_2E_0/p\ell$ decrease with increasing the parameter E_1/E_0. The difference between the values obtained for Case 0 and the other Cases also increase with the size of the hole.

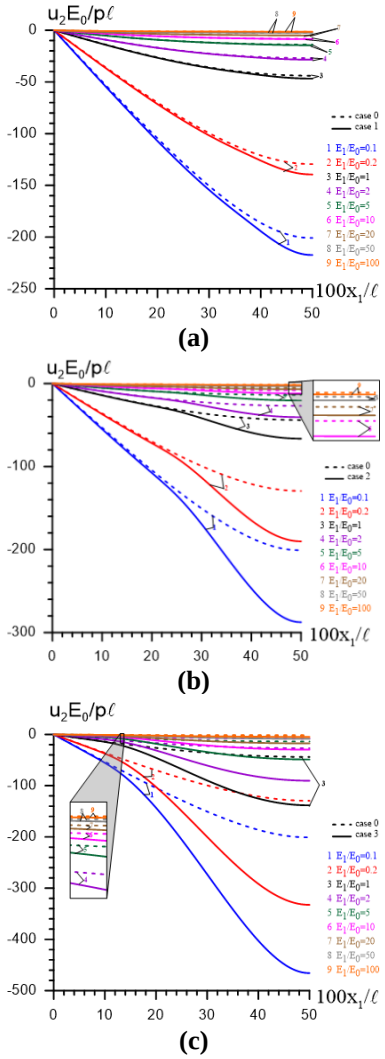

Figure 12. The normalized displacement of $u_2E_0/p\ell$ at x_2=h plane for different values of E_1/E_0 for n=2 for (a) Case 1 (b) Case 2 (c) Case 3 versus Case 0 for Problem 1.

The effect of power-law exponent value, (i.e., n) on the displacement distribution of $u_1E_0/p\ell$ $(u_2E_0/p\ell)$ for three cases versus Case 0 on the plane x_2=h for Problem 1 are plotted in Figure 13 (Figure 14). As can be seen from the graphs, the absolute values of displacements increase rapidly at the sharp corners of the hole. It follows from the graphs that the absolute values of the displacements increase with increasing the parameter n. The difference between the values obtained for Case 0 and the other Cases also increase with the size of the hole. The presence of hole increases the effect of n.

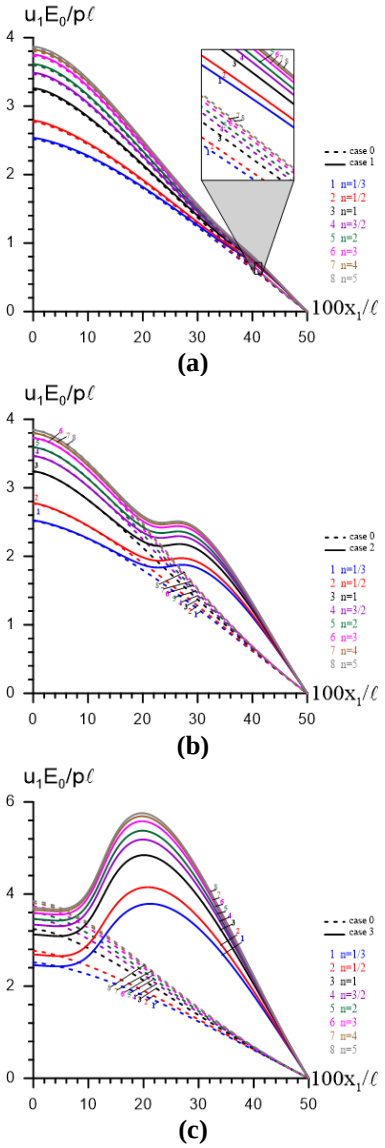

Figure 13. The normalized displacement of $u_1E_0/p\ell$ at x_2=h plane for different values of n for $E_1/E_0=5$ for (a) Case 1 (b) Case 2 (c) Case 3 versus Case 0 for Problem 1.

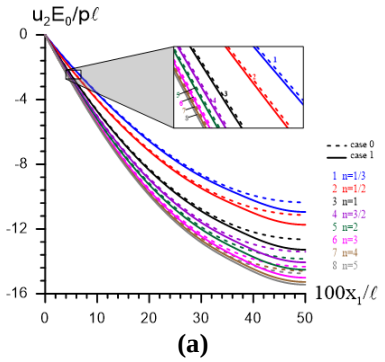

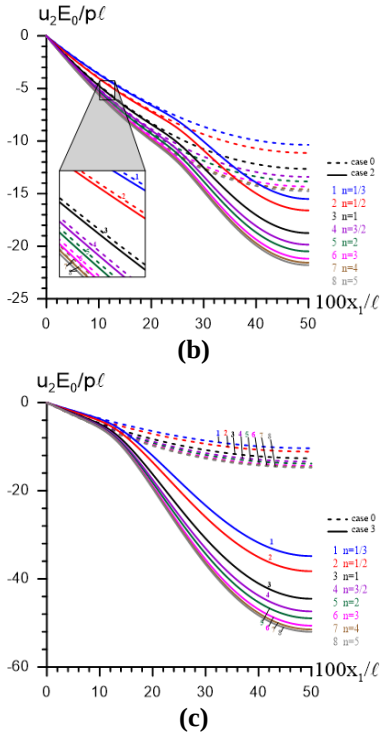

Figure 14. The normalized displacement of $u_2E_0/p\ell$ at x_2=h plane for different values of n for $E_1/E_0=5$ for (a) Case 1 (b) Case 2 (c) Case 3 versus Case 0 for Problem 1.

The effect of power-law exponent value, (i.e., n) on the displacement distribution of $u_2E_0/p\ell$ for three cases versus Case 0 on the plane $x_1=\ell_s/2$ for Problem 2 are plotted in Figure 15. It follows from the graphs that the absolute values of the displacements increase with increasing the parameter n.

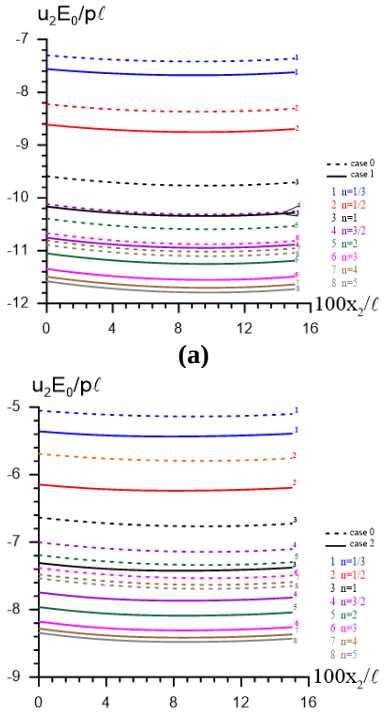

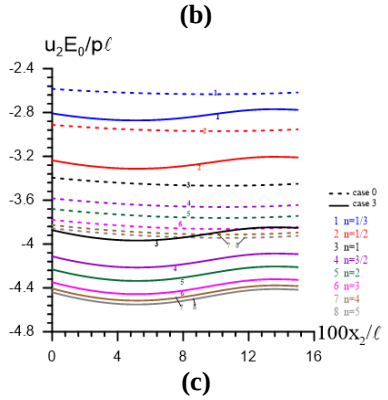

Figure 15. The normalized displacement of $u_2E_0/p\ell$ at $x_1=\ell_s/2$ plane for different values of n for $E_1/E_0=5$ for (a) Case 1 (b) Case 2 (c) Case 3 versus Case 0 for Problem 2.

5. Conclusions

A static analysis of a plate-strip made of functionally-graded material (FGM) containing a rectangular hole has been investigated under bending forces. The plate-strip is simply supported at two opposite ends. Classical linear elasticity theory and the generalized plane-strain conditions are used to analyze the problem. The plate-strip's material is assumed functionally graded. Using the FEM, effect of grading direction, power-law exponent, size of the hole and magnitude of material nonhomogeneity parameter on the displacements and the stresses have been investigated. From the numerical results, the following conclusions can be drawn:

- The difference between the values of stresses and displacements obtained for unholed medium (Case 0) and holed medium (the other Cases) increase with the size of the hole as the ratio E_1/E_0 changes,
- The more E_1/E_0, the larger absolute values of the stresses of σ_{11}/p for Problem 1 (Figure 5),
- As the size of the hole increases, the difference between the values of the stresses for FGM and homogeneous plate (E_1/E_0=1) increases (Figure 5-9),
- For the ratio E_1/E_0=1 in which the FGM plate becomes a homogeneous plate, the stress concentration is a linear function of x_2 and the maximum stress of σ_{11}/p is at the top or bottom surface of the plate for Case 1 and Case 2, but for Case 3 it is not

linear because of the hole effect (Figure 6).

- The most affected stress by the change of E_1/E_0 is σ_{11}/p for both problems.
- The absolute values of the displacements decrease with increasing the parameter E_1/E_0 (Figure 10-12).
- The absolute values of the displacements increase with increasing the parameter n in direction of x_1 and x_2 (for both problems). The presence of hole increases the effect of n (Figure 13-15).

References

[1] Savin GN. Stress concentration around holes. Oxford: E. Gros Translator, Pergomon; 1961.

[2] Jong TD. Stress around rectangular holes in orthotropic plates, Journal of Composite Materials 1981; 15(4): 311-328.

[3] Rao DKN., Babu MR., Reddy KRN., Sunil D. Stress around square and rectangular cutouts in symmetric laminates, Composite Structures 2010; 92(12): 2845-2859.

[4] Lei GH., Charles WWN., Rigby DB. Stress and displacement around an elastic artifical rectangular hole, Journal of Engineering Mechanics 2001; 127(9): 880-890.

[5] Yahnioğlu N., Yücel MA. Dikdörtgen delik formunda dolgu malzemesi içeren şerit levhada gerilme birikimi, YTÜ Dergisi 2002; 4(7): 67-77.

[6] Erdogan F., Wu BH. The surface crack problem for a plate with functionally graded properties, Journal of Applied Mechanics 1997; 64(3): 449-456.

[7] Santare MH., Lambros J. Use of graded finite elements to model the behavior of nonhomogeneous materials, Journal of Applied Mechanics 2000; 67(4): 819-822.

[8] Kim JH., Paulino GH. Isoparametric graded finite elements for nonhomogeneous isotropic and orthotropic materials, Journal of Applied Mechanics 2002; 69(4): 502-514.

[9] Udupa G., Rao SS., Gangadharan KV. Functionally graded composite materials: an overview, Procedia Materials Science 2014; 5: 1291-1299.

[10] Goyat V., Verma S., Garg RK. Reduction of stress concentration for a rounded rectangular hole by using a functionally graded material layer, Acta Mechanica 2017; 228(10): 3695-3707.

[11] Zienkiewicz OC., Taylor RL. The finite element methods: basic formulation and linear problems 4th Ed. Oxford: Mc Graw-Hill Book Company; 1989.

[12] Timoshenko SP., Goodier JN. Theory of elasticity 3rd edition. London, Mc: Graw-Hill International Editions; 1970.